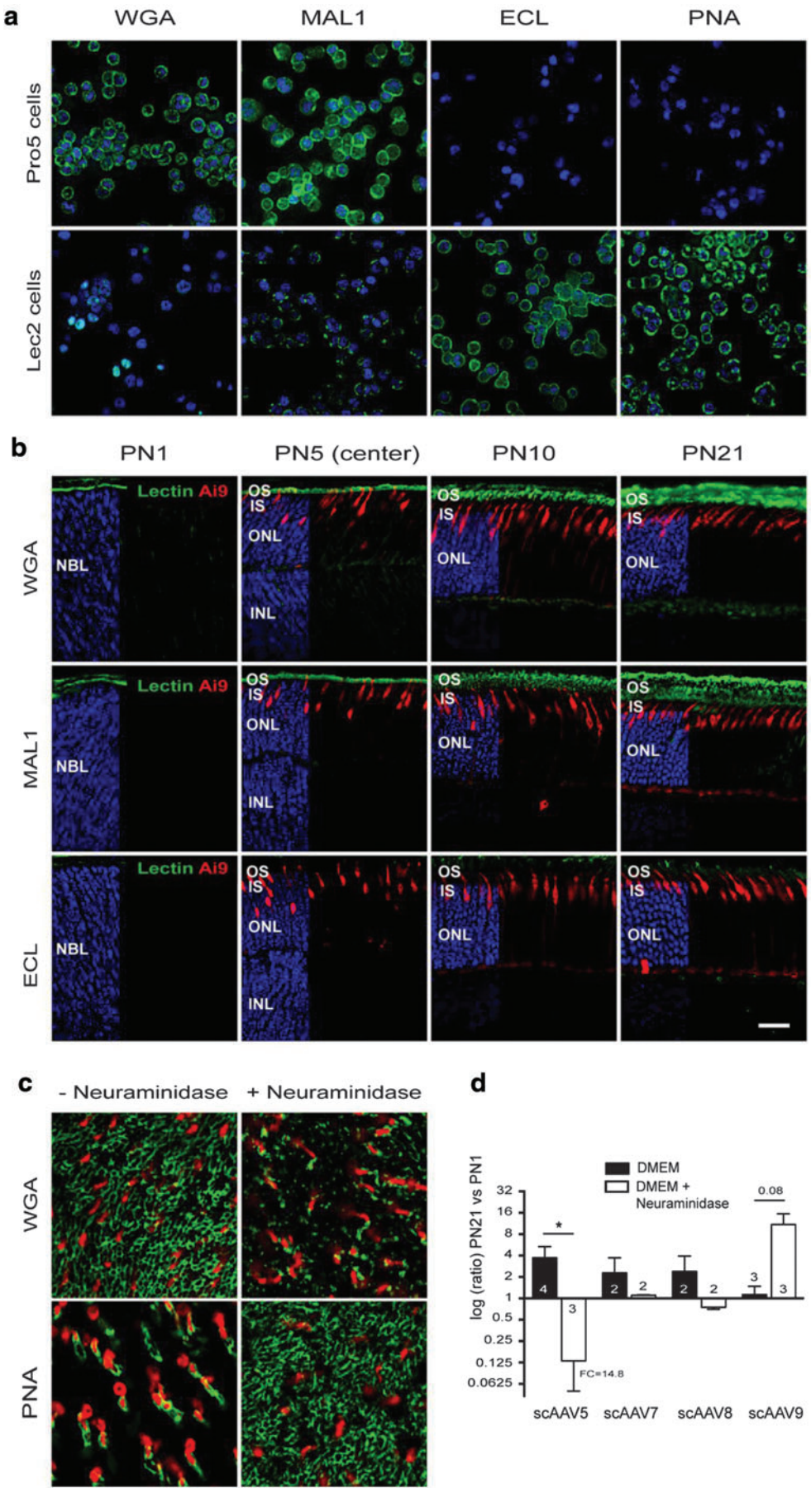
a
WGA
MAL1
ECL
PNA
Pro5 cells
Lec2 cells
b
PN1
PN5 (center)
PN10
PN21
WGA
MAL1
ECL
Lectin Ai9
NBL
OS
IS
ONL
INL
c
- Neuraminidase
+ Neuraminidase
WGA
PNA
d
DMEM
DMEM + Neuraminidase
log (ratio) PN21 vs PN1
32
16
8
4
2
1
0.5
0.25
0.125
0.0625
*
0.08
FC=14.8
4
3
2
2
2
2
3
3
scAAV5
scAAV7
scAAV8
scAAV9

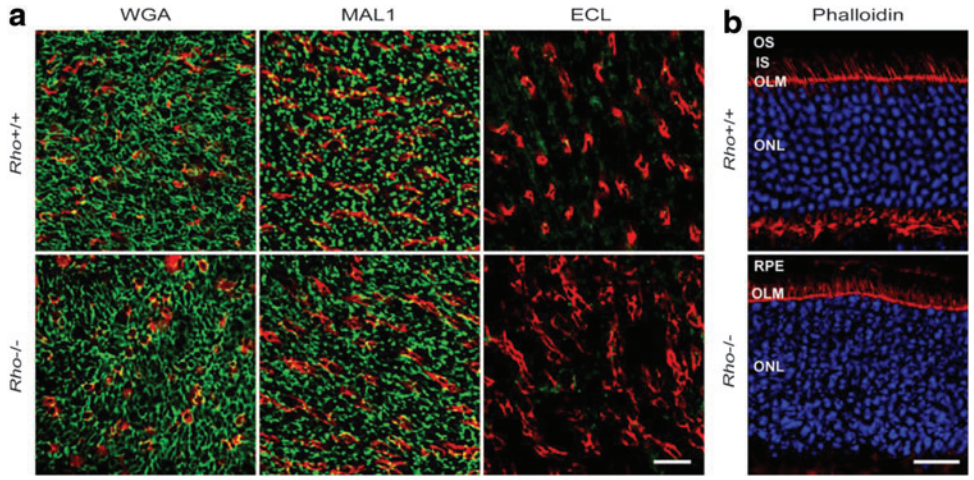

Supplementary Figure S9. Histological analysis of the inter-photoreceptor matrix (IPM) and outer limiting membrane (OLM) integrity in PND21 *Rho*$^{-/-}$ mice. **(a)** Retinal flat mounts of PND21 *Rho*$^{-/-}$ and *Rho*$^{+/+}$ mice were labeled with Cy3-PNA (*red*) and fluorophore-conjugated WGA, MAL1, or ECL (*green*). Representative images are shown of experiments run in duplicate. Despite absence of rod outer segments, no change of the rod IPM structure is apparent at PND21 in *Rho*$^{-/-}$ mice. Slight swelling of cone matrix sheaths is observed. **(b)** Retinal cryosections of PND21 *Rho*$^{-/-}$ and *Rho*$^{+/+}$ mice were labeled with Cy3-Phalloidin (which labels F-actin; *red*) and counterstained with DAPI (*blue*). Despite the absence of rod outer segments, no disruption of the OLM integrity is apparent at PND21 in *Rho*$^{-/-}$ mice. Scale bars = 25 μm.

Supplementary Figure S8. Analysis of IPM formation in the developing mouse retina and its interactions with AAV particles. To address the possibility that the IPM influences the transduction of PRs, first the development of the IPM in the mouse retina was examined from PND1 to PND21 using four different lectins: WGA (a sialic-acid terminal sugar-specific lectin), MAL1 (a Sia[α2,3]-Gal[β1,4]GlcNAc and Gal[β1,4]GlcNAc terminal sugar-specific lectin), ECL (a Gal[β1,4]GlcNAc terminal sugar-specific lectin), and PNA (a Gal[β1,4]GlcNac terminal sugar-specific lectin). **(a)** To verify the specificity of the lectins, *Pro5* (*upper panels*) and *Lec2* (*lower panels*) CHO cell lines were stained with fluorophore-conjugated WGA, MAL1, ECL, and PNA lectins (*green*). DAPI labels the cell nuclei (*blue*). *Lec2* cells lack terminal sialic acids due to a defect in CMV-sialic acid transport and express at their surface glycans with terminal galactosyl residues. As expected, *Pro5* cells expressing sialylated glycans demonstrate preferential staining with WGA and MAL1. In contrast, *Lec2* cells demonstrate preferential staining by ECL and PNA. **(b)** Retinal cross sections of PND1, PND5, PND10, and PND21 *Ai9_MCre*$^{+}$ (labeling cones by td-Tomato; *red*) mice were labeled with fluorophore-conjugated WGA, MAL1 or ECL (*green*) and counterstained with DAPI (*blue*). The sections show the increase of IPM during photoreceptor development. The different lectins confirm the presence of rod and cone IPM microenvironments with specific glycan compositions. WGA and MAL1 are specifically bound to the rod-associated IPM only. In contrast, only glycoproteins with terminal Gal and GlcNAc residues are detectable in the mouse cone matrix sheaths and outer segments, as assessed by specific labeling using PNA and ECL. **(c and d)** Effect of neuraminidase treatment on AAV binding to *ex vivo* retinal explants. *Ex vivo* retinal explants were used to limit the variability related to the surface of the retina exposed to the vectors after subretinal injections at PND1 versus PND21. Retinal explants were pretreated with DMEM alone or DMEM plus neuraminidase and incubated with the same dose of AAV5, –7, –8, and –9. **(c)** Loss of terminal Sia residues upon neuraminidase treatment was confirmed using WGA and PNA binding (*green*) in *Ai9*$^{+}$*_MCre*$^{+}$ adult retinas that specifically expressed td-Tomato in cones (*red*). As expected, a reduction in WGA labeling of the rod-associated IPM was observed, as well as the extension of PNA staining to both cone and rod IPM domains. **(d)** AAV binding on PND21 retinal explants was quantified by qPCR and compared to the binding obtained on PND1 retinal explants. All experiments were carried out in triplicate. Results are shown as mean ± *SD*. Numbers in bars represent the number of retina analyzed. AAV particle binding to untreated control retinas was significantly increased from PND1 to PND21 for AAV2/5 (3.72-fold change), AAV2/7 (2.28-fold change), AAV2/8 (2.38-fold change), but not for AAV9. Neuraminidase treatment abrogated the increase of AAV5 binding over time, without affecting AAV7 and AAV8 binding. In contrast, hydrolysis of sialic acid residues increased AAV9 binding over time by 10.9-fold. These results are in agreement with previous work showing that (α2,3) N-linked Sia[51–53] and terminal galactose[54, 55] may mediate AAV5 and AAV9 transduction, respectively. They suggest that the rod-associated matrix selectively binds AAV5 while masking glycans that facilitate AAV9 binding *in vitro*. Notably, these differences in AAV binding to the IPM did not denote a significant different capacity of transducing mouse PRs *in vivo* at PND21, considering the percentage of cell transduced. *$p < 0.05$ by Student's *t*-test. Scale bar = 25 μm. FC, fold-change.